

The Effect of BN Content on the Thermal Expansion Properties of SiC Composite Ceramics

Weijing Kong, Bin Hu*

College of Physics and Electrical Engineering, Kashgar University, Kashgar 844000
received December 29, 2024; received in revised form February 10, 2025; accepted December 11, 2025

Abstract

Silicon carbide (SiC) ceramics are a novel packaging material that has demonstrated significant potential in the field of electronic packaging in recent years. In this study, SiC composite ceramics were prepared using a pressureless liquid-phase sintering method with Al_2O_3 - Y_2O_3 - MgO -BN as sintering additives. The influence of the BN content on the thermal properties of SiC composite ceramics was investigated, with the aim of exploring the performance advantages of SiC composite ceramics in packaging applications. The results indicate that the main crystalline phase of all samples is 6H-SiC, with a relatively uniform grain size distribution ranging between 0–2 μm . The sample with a mass ratio of 90%SiC:2% Al_2O_3 :3% Y_2O_3 :2% MgO :3%BN (labeled as M2B3) exhibited a hardness of 340.22 N/mm^2 , thermal expansion coefficient of $3.35 \times 10^{-6} \text{ K}^{-1}$, dielectric constant of $\epsilon = 486.211$, and dielectric loss of $\tan \delta = 0.507$. These properties meet the requirements for high hardness, low dielectric loss, and well-matched thermal expansion coefficient, making SiC composite ceramics a promising candidate for next-generation high-performance electronic packaging materials.

Keywords: Silicon carbide composite ceramics, coefficient of thermal expansion, dielectric constant, dielectric loss

I. Introduction

With the rapid development of the electronics industry, there is an increasing demand for cost-effective, high-performance packaging materials. It is essential for an electronic packaging material to possess a relatively matched thermal expansion coefficient, excellent electrical properties, mechanical strength, and environmental adaptability to meet the growing complexity and multifunctionality of modern electronic devices^{1–4}. An ideal electronic packaging substrate requires high thermal conductivity and effective heat dissipation to prevent thermal damage to the chips. Additionally, a low dielectric constant and low dielectric loss are essential characteristics to facilitate the efficient transmission of high-frequency signals. Moreover, a low coefficient of thermal expansion (CTE) is crucial to ensure compatibility with Si or GaAs chips, thereby avoiding thermal stress caused by mismatched thermal expansion during operation, as this could lead to chip failure^{5–6}.

In recent years, with advancements in fabrication techniques and cost reduction, the application of silicon carbide (SiC) ceramics in the field of electronic packaging has gradually increased. As a wide-bandgap semiconductor material, SiC ceramics have attracted significant attention on account of their excellent properties, including high-temperature resistance, corrosion resistance, radiation resistance, good thermal stability, high thermal conductivity, and low coefficient of thermal

expansion^{7–11}. However, SiC is a typical strong covalent compound, with the ionicity of Si-C bonds being only about 12%. This results in an extremely low self-diffusion coefficient at high temperatures¹². Consequently, pure SiC ceramics are difficult to sinter under normal conditions, and the preparation process typically requires the use of sintering additives.

Researchers commonly use Y_2O_3 , Al_2O_3 , and MgO as sintering additives^{13–19}, which not only promote the sintering of SiC ceramics but also enhance the density and mechanical properties of the ceramic materials. However, for SiC ceramics to be suitable for electronic packaging applications, they not only need to exhibit good densification and mechanical properties but also possess excellent electrical properties and an appropriate coefficient of thermal expansion. Studies by Cai *et al.*²⁰ have shown that boron nitride (BN), thanks to its wide bandgap, high thermal conductivity, exceptional strength, good flexibility, and excellent thermal and chemical stability, is a strong candidate for thermal management applications. Malik *et al.*²¹ found that the addition of BN as a sintering aid in SiC ceramics not only improves their fracture toughness but also reduces the electrical resistivity of the ceramics. Furthermore, Kultayeva *et al.*²² demonstrated that a certain amount of BN can enhance not only the mechanical properties, such as toughness, but also the electrical and thermal performance of SiC ceramics.

Based on the above analysis, in this study silicon carbide (SiC) composite ceramics were synthesized using Al_2O_3 - Y_2O_3 - MgO -BN as sintering additives and SiC powder at

* Corresponding author: 1508041566@qq.com

1850 °C under an inert argon atmosphere. The effects of varying BN content on the microstructure, coefficient of thermal expansion (CTE), and dielectric properties of the SiC composite ceramics were systematically investigated.

II. Experiments

(1) Experimental materials

The starting materials were commercially available high-purity α -silicon carbide (purity 99.90 %; density 3.21 g/cm³), yttrium oxide (purity 99.99 %; density 5.02 g/cm³), aluminum oxide (purity 99.99 %; density 1.06 g/cm³), magnesium oxide (purity 99.99 %; density 3.57 g/cm³), boron nitride (purity 99.90 %; density 2.27 g/cm³) powders.

(2) Sample preparation

The SiC ceramics were prepared with a pressureless sintering method. Initially, SiC and sintering additives were weighed according to the mass ratios listed in Table 1. The mixture was then milled in a planetary ball mill for 24 hours, and then dried. Subsequently, the dried powder was pressed into pellets on a manual tablet press. After debinding, the samples were sintered in a vacuum carbon tube furnace. The sintering process was conducted at 1850 °C with a holding time of 2 hours, under a continuous argon atmosphere for protection. After sintering, the samples were cooled down naturally inside the furnace to obtain the final ceramic products.

Table 1: Sample number and formula.

Number	SiC	Al ₂ O ₃	Y ₂ O ₃	MgO	BN
M4B1	90 %	2 %	3 %	4 %	1 %
M3B2	90 %	2 %	3 %	3 %	2 %
M2.5B2.5	90 %	2 %	3 %	2.5 %	2.5 %
M2B3	90 %	2 %	3 %	2 %	3 %
M1B4	90 %	2 %	3 %	1 %	4 %

(3) Sample characterization

The crystalline phases of the ceramic samples were analyzed using an X-ray diffractometer (XRD, DX-2600, Dandong Fangyuan Instrument Co., Ltd.). The analysis was conducted with Cu K α radiation over a 2θ range of 20 ° to 80 ° at a scanning rate of 0.03 °/min. The surface morphology of the ceramics was observed using a scanning electron microscope (SEM, KYKY-2800B, Zhongke Keyi). The thermal expansion coefficient of the samples was measured using a thermal expansion instrument (CTE, DIL402C, Netzsch, Germany). The measurements were performed in a helium atmosphere, with fused silica as the baseline reference, over a temperature range of -150 °C to 500 °C at a heating rate of 5 K/min. The impedance of the SiC composite ceramic samples was measured using a precision impedance analyzer (E4990A). Prior to the impedance measurements, the samples were ground, polished, and coated with silver.

The measurements were conducted at room temperature with a frequency of 10⁶ Hz.

III. Results and Discussion

(1) Analysis of the measurement results for SiC-Al₂O₃-Y₂O₃-MgO-BN composite ceramic structure

Fig. 1 shows the XRD patterns of SiC composite ceramic samples with different sintering additive ratios compared with pure SiC powder. As shown in Fig. 1, the diffraction peaks of all samples are sharp and well-defined, with the main crystalline phase being 6H-SiC²³. With the addition of a small amount of B³⁻ (sample M4B1), no secondary phases were detected within the measurement range, indicating that Y₃Al₅O₁₂ and BN have successfully entered the 6H-SiC lattice to form a solid solution. However, as the BN content increases, the diffraction peaks of B-containing compounds (such as Mg₂B₂O₅ and Mg(B₁₂)C₂), N-containing compounds (such as Al₆C₃N₂), Mg-containing compounds (such as Mg₂SiO₄), and Al- and Y-containing compounds (such as Y₃Al₅O₁₂) gradually become more pronounced. This phenomenon may be attributed to the following: at high temperatures, with the increase in B³⁻ and N³⁺ content and the decrease in Mg²⁺ content, a certain amount of Mg²⁺, B³⁻, and N³⁺ can further promote the formation of new characteristic peaks corresponding to the Y₃Al₅O₁₂ compound. Y₃Al₅O₁₂ is a low-melting-point liquid phase, and its formation reaction can be described by the following equations^{24–25}:

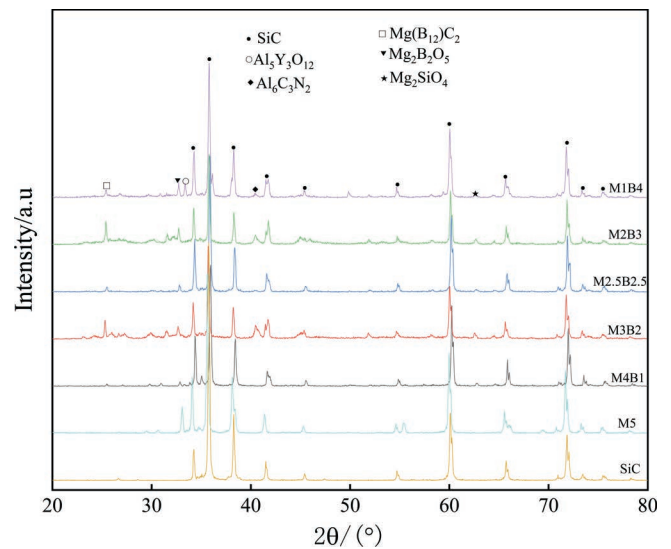
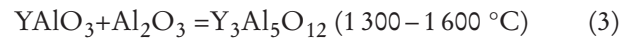
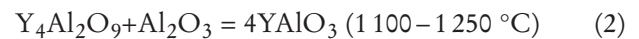
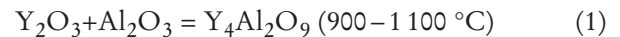


Fig. 1: XRD patterns of SiC-Al₂O₃-Y₂O₃-MgO-BN ceramics and SiC powder in a silicon carbide ceramic with different ratios.

(2) Microscopic morphology measurement results and analysis of SiC-Y₂O₃-Al₂O₃-MgO-BN composite ceramic

Fig. 2 presents the SEM images of SiC composite ceramic samples sintered with different ratios of sintering additives (Al₂O₃-Y₂O₃-MgO-BN). As shown in Fig. 2, with the

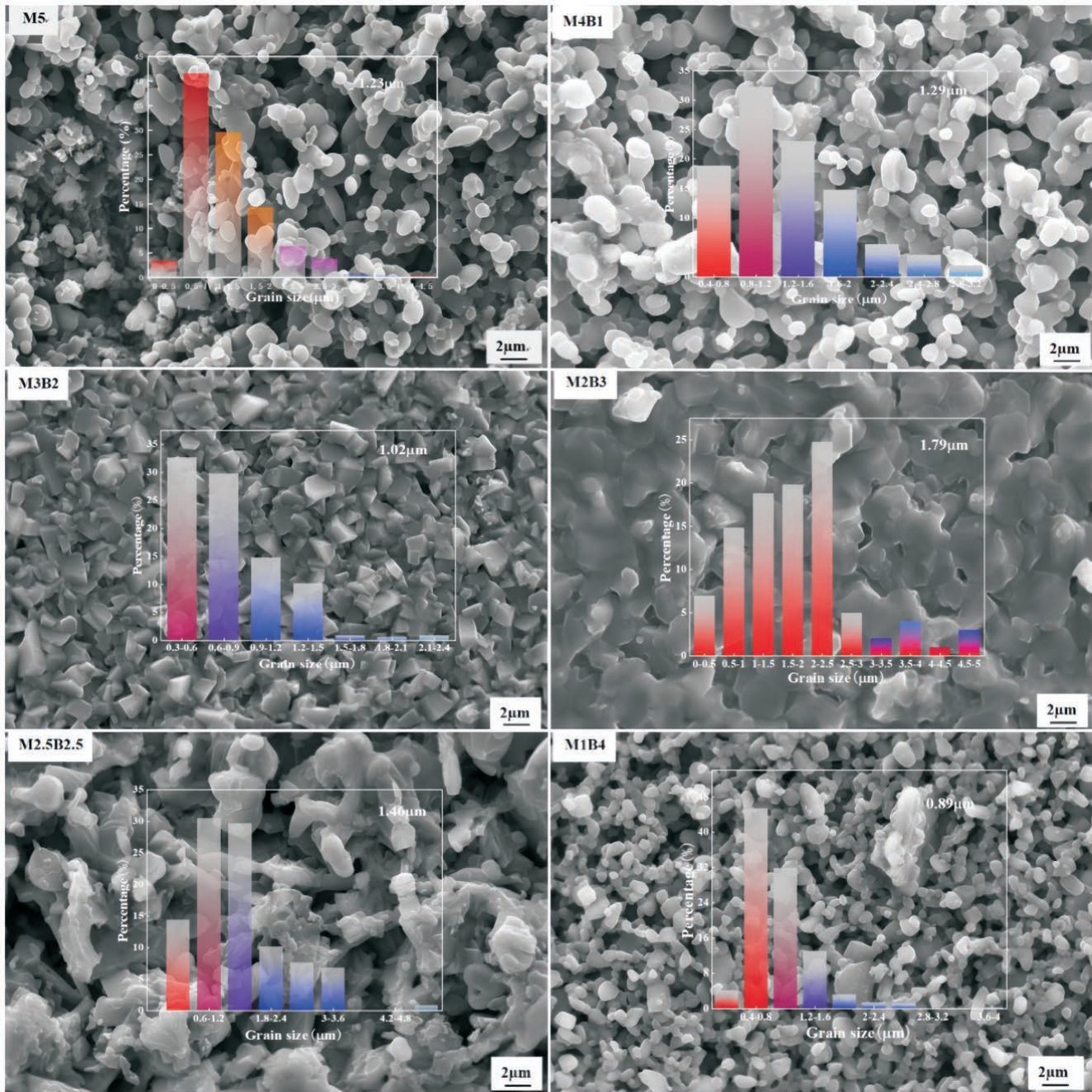


Fig. 2: SEM microstructures of SiC-Al₂O₃-Y₂O₃-MgO-BN ceramic after sintering.

increase in BN content, distinct grain boundaries and irregularly shaped grains are observed in the samples. Some of the SiC composite ceramic samples exhibit grain bonding phenomena. From a comparison of the images, it is evident that as the BN content in the sintering additives gradually increases, the average grain size initially increases and then decreases. Samples M2B3 and M3B2 show fewer pores, with the M2B3 sample exhibiting a liquid-phase state, making it the densest among the series of SiC ceramics. From a combination of these results with those of XRD analysis, it can be concluded that when the BN content reaches 3 %, Al₂O₃ reacts fully with Y₂O₃, MgO with BN, and MgO with SiO₂, generating bonding phases that enhance densification, which is consistent with the SEM results.

(3) Analysis of mass loss in samples after sintering

Fig. 3 presents the data on hardness and linear shrinkage of SiC ceramic samples with different compositions, analyzed in conjunction with the values shown in Table 3. The results indicate that all SiC ceramic samples exhibited varying degrees of mass loss and linear shrinkage. On the basis of a comparison, it can be concluded that as the BN content increases, the linear shrinkage rate of the silicon carbide composite ceramic samples shows a decreasing trend, while the hardness initially increases and then decreases. From a combination of scanning electron microscopy analysis, it is evident that the different ratios of sintering aids lead to the combined effects of ceramic powder particle size and grain distribution²⁶. The uneven distribution of particle sizes and the presence of pores

influence the hardness of SiC ceramics. BN can enhance the hardness of silicon carbide composite ceramics. The M2B3 ceramic sample, for instance, demonstrates a relatively high hardness value of 340.22 N/mm², with a mass loss of 0.1203 g and a linear shrinkage rate of 5.2 %.

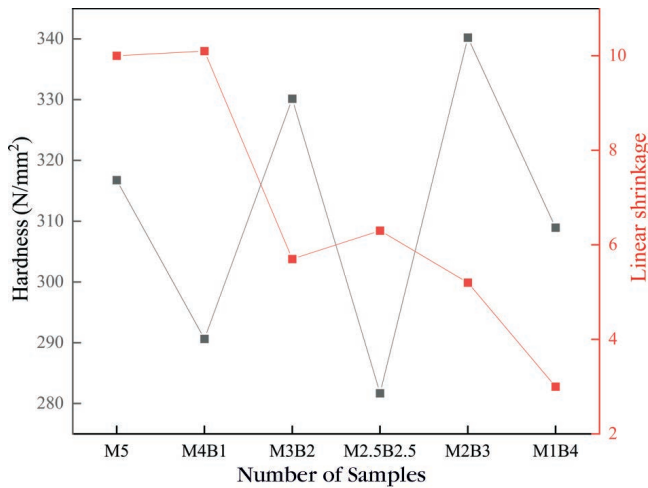


Fig. 3: Data on hardness and linear shrinkage of SiC ceramic.

(4) Thermal expansion analysis

Fig. 4 illustrates the linear shrinkage (a) and coefficient of thermal expansion (CTE) (b) of silicon carbide composite ceramics with different ratios of sintering aids as a function of temperature. From graph (b), it can be observed that each curve exhibits an inflection point, which corresponds to the minimum CTE. As the BN content increases, the minimum CTE transitions from positive to negative and then back to positive,

indicating that a certain amount of BN can reduce the CTE of silicon carbide composite ceramics²⁷. Combined with microstructural morphology and phase analysis, the reason for this phenomenon may be attributed to the anisotropic nature of BN grains influencing the thermal expansion properties²⁸. With increasing BN content, the MgO in the samples reacts with SiO₂ and BN, forming a liquid phase and causing an increase in atomic thermal vibration. When the interatomic distance increases, the enhanced vibration distance is partially accommodated, resulting in a lower CTE on a macroscopic scale. Based on the data in Table 3, BN can effectively reduce the CTE of silicon carbide composite ceramics. When the sintering aid ratio is M3B2, the ceramic sample exhibits the lowest CTE of $7.37 \times 10^{-7} \text{ K}^{-1}$. However, for applications as electronic packaging substrates, the material's CTE must match that of silicon ($3.5 \times 10^{-6} \text{ K}^{-1}$)²⁹. In this regard, the M2B3 material shows better compatibility.

Table 2: The hardness, mass loss and linear shrinkage of different ratio ceramic samples at 1850 °C sintering temperature.

Temperature	Hardness/ N/(mm ²)	Mass loss/g	Linear shrinkage
M4B1	290.6327	0.1125	10.1 %
M3B2	330.1633	0.1276	5.7 %
M2.5B2.5	281.6939	0.1564	6.3 %
M2B3	340.2245	0.1203	5.2 %
M1B4	308.9490	0.1453	3.0 %

Table 3: Thermal expansion coefficients of SiC-Al₂O₃-Y₂O₃-MgO-BN ceramic samples with different sintering aid ratios.

Sintering aid	M4B1	M3B2	M2.5B2.5	M2B3	M1B4
Thermal expansion coefficient·K ⁻¹	3.16946×10^{-6}	7.36586×10^{-7}	1.17185×10^{-6}	3.35432×10^{-6}	3.65602×10^{-6}

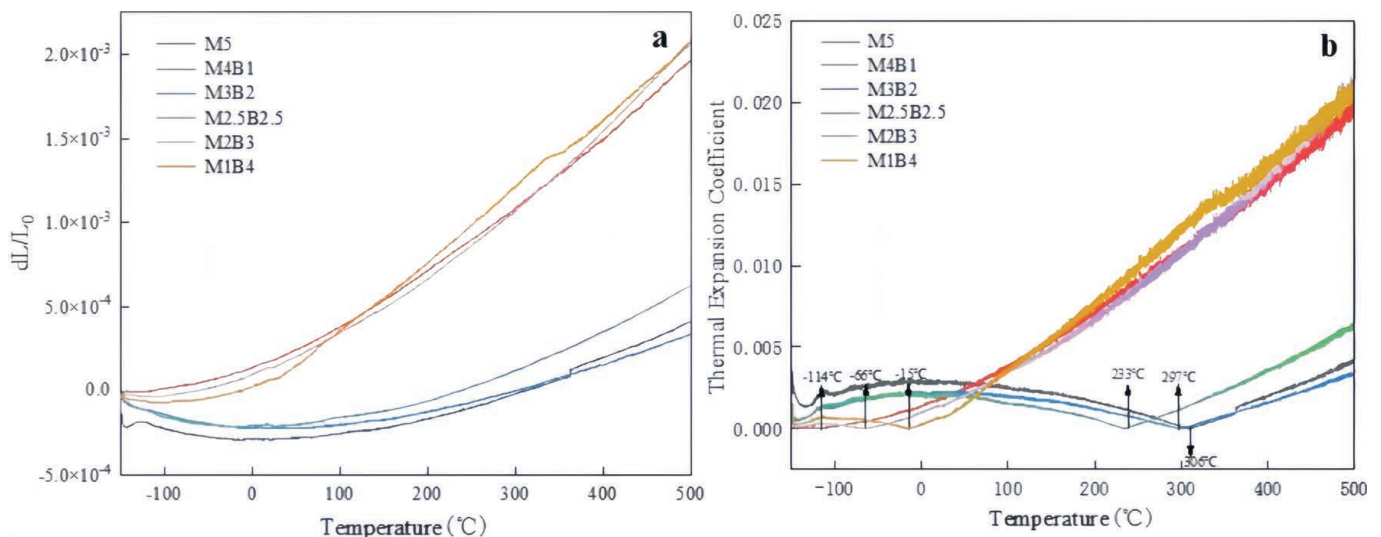


Fig. 4: Linear shrinkage and coefficient of thermal expansion of silicon carbide ceramics with temperature under different sintering aid ratios.

(5) Dielectric property analysis of SiC-Al₂O₃-Y₂O₃-MgO-BN ceramic

Fig. 5 presents a comparison of the relative permittivity and dielectric loss of silicon carbide composite ceramics with varying contents of sintering aids. As shown in Fig. 5, the relative permittivity of each sample initially decreases and then stabilizes with increasing BN content. This phenomenon may be attributed to the combined effects of particle size and grain distribution on the ceramic surface. Based on SEM analyses, the uneven distribution of particle sizes resulting from different ratios of sintering aids may influence the complexity of the SiC ceramic interface, thereby affecting the interfacial polarization of the composite material³⁰. The sample M2B3 exhibits a relative permittivity of $\epsilon = 486.211$ and a dielectric loss of $\tan \delta = 0.507$, indicating that it is a promising silicon carbide composite ceramic material with low dielectric loss.

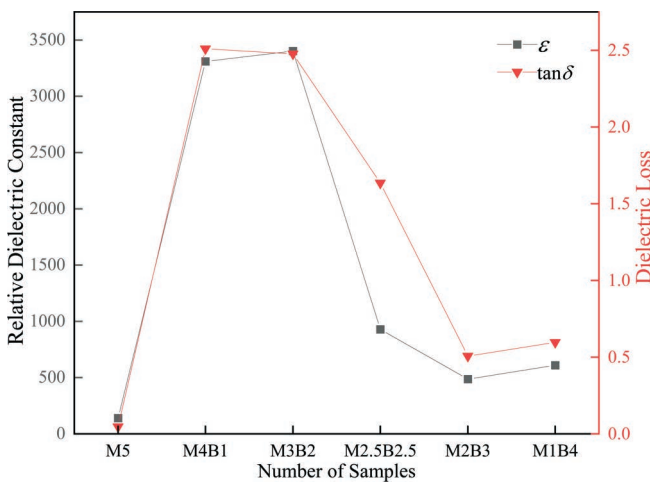


Fig. 5: Comparison of relative permittivity and dielectric loss of sintering aids with different proportions.

IV. Conclusions

A series of SiC-Al₂O₃-Y₂O₃-MgO-BN composite ceramics prepared with different ratios of sintering aids were subjected to structural, morphological, thermal, and dielectric analyses. The following conclusions were drawn: With the increase in BN content, the main crystalline phase of all silicon carbide composite ceramic samples remained 6H-SiC, and new characteristic peaks were observed in each sample. In a comparison of the coefficients of thermal expansion (CTE), it was found that BN can effectively reduce the CTE of silicon carbide ceramics to some extent. The sample M3B2 exhibited the lowest CTE, with a value of $7.36586 \times 10^{-7} \text{ K}^{-1}$. The relative permittivity of the samples gradually decreased with increasing BN content under different sintering aid ratios. The sample M2B3 showed the lowest relative permittivity, with $\epsilon = 486.211$ and a dielectric loss of $\tan \delta = 0.507$ at a frequency of 10^6 Hz .

Acknowledgement

This work was supported by the Kashgar Regional Science and Technology Plan Project (Grant No.

KS2022093) and the Kashgar University Institutional Project (Grant No. (2021) 2740).

References

- He, R., Zhou, N., Zhang, K. *et al.*: Progress and challenges towards additive manufacturing of SiC ceramic, *J. Adv. Ceram.*, **10**, [4], 637–674, (2021).
- Liang, Z., Zhang, H., Li, Y. *et al.*: A reverse particle grading strategy for design and fabrication of porous SiC ceramic supports with improved strength, *J. Adv. Ceram.*, **13**, [7], 1011–1022, (2024).
- Du, Z., Yi, M., Shi, B. *et al.*: Strengthening and toughening of CNTs-reinforced B₄C-SiC ceramic composite material via spark plasma sintering, *Int. J. Appl. Ceram. Tec.*, **20**, [6], 3691–3700, (2023).
- Lamon, J.: Investigation of variability of flaw strength distributions on brittle SiC ceramic, *Ceramics*, **7**, [2], 2571–6131, (2024).
- Song, W.: Research status of ceramic substrate materials for electronic packaging, *Powder Sci. Technol.*, (04), 25–27, (2019).
- Zhang Wenyu: Research and application of electronic packaging materials, *J. Shanghai Electr. Technol.*, **10**, [02] 72–77, (2017).
- Wang, W., Jia, J., Sun, Y. *et al.*: The microstructure evolution process and flexural behaviours of SiC matrix ceramic infiltrated by aluminium base alloy, *Materials*, **15**, [16], 5746, (2022).
- Li, H.W., Zhao, Y.P., Chen, G.Q. *et al.*: SiC-based ceramics with remarkable electrical conductivity prepared by ultrafast high-temperature sintering, *J. Eur. Ceram. Soc.*, **43**, [5], 2269–2274, (2023).
- Wang, C., Wu, S., Yan, C. *et al.*: Research and applications of additive manufacturing technology of SiC ceramics, *Sci. Bull.*, **67**, [11], 1137–1154, (2022).
- Kumar, D., Rajak, S.K., Seetharam, R. *et al.*: Effect of Y₂O₃ additive on mechanical and wear behaviour of hBN reinforced SiC ceramic matrix composite, *Materials Today Proc.*, **87**, 193–196, (2023).
- Gupta, K., Murtaza, Q., Yuvraj, N.: Development of ZrB₂-SiC plasma-sprayed ceramic coating for Thermo-chemical protection in hypersonic vehicles, *J. Mater. Eng. Perform.*, **33**, [3], 1401–1410, (2024).
- Johnson, J.A., Hrenya, C.M., Weimer, A.W.: Intrinsic reaction and self-diffusion kinetics for silicon carbide synthesis by rapid carbothermal reduction, *J. Am. Ceram. Soc.*, **85**, [9], 2273–2280, (2022).
- Zang, X., Li, H., Lu, Y. *et al.*: Dielectric properties and thermal conductivity of Si₃N₄-SiC composite ceramics, *J. Korean Ceram. Soc.*, **59**, 903–908, (2022).
- Ren, L.K., Ren, Q.X., Yin, Z.Q. *et al.*: Li₂O addition as a means of achieving low-temperature densification of SiC ceramic, *Ceram. Int.*, **50**, 39440–39447, (2024).
- Dioktyanto, M, Aryanto, D., Noviyanto, A., Yuwono, A.H., Rochman, N.T.: Enhancing the density of silicon carbide with the addition of nitrate-based additives, *J. Min. Metall. B: Metall.*, **58**, [3], 389–395, (2022).
- Zhang, S., Wang, J., Zhang, M. *et al.*: Mechanical and tribological behaviors of hot-pressed SiC/SiCw-Y₂O₃ ceramics with different Y₂O₃ contents, *Coatings*, **13**, [5], 956, (2023).
- Zhu, Y., Qin, Z., Chai, J. *et al.*: Effects of sintering additives on microstructure and mechanical properties of hot-pressed α -SiC ceramics, *Metall. Mater. Trans. A.*, **53**, [4], 1188–1199, (2022).
- Fu, Q., Yang, Y., Wang, J. *et al.*: Silicon carbide ceramics manufactured by digital light processing and low temperature sintering, *Ceram. Int.*, **50**, [19], 36892–36899, (2024).

- ¹⁹ Yun, S.I., Nahm, S., Park, S.W.: Effects of the size distribution of SiC powders on the microstructures and properties of liquid phase bonded porous SiC with neck bonding phases of $Y_4Al_2O_9$, $Y_3Al_5O_{12}$, $Y_2Si_2O_7$, and Al_2O_3 , *J. Ceram. Soc. Jpn.*, **129**, [11], 660–668, (2021).
- ²⁰ Qiran, C., Declan, S., Wei, G. *et al.*: High thermal conductivity of high-quality monolayer boron nitride and its thermal expansion, *Science Advances*, **5**, [6], 2375–2548, (2019).
- ²¹ Malik, R., Kim, Y.W.: Pressureless solid-state sintering of SiC ceramics with BN and C additives, *J. Asian Ceram. Soc.*, **15**, 1–8, (2021).
- ²² Kultayeva, S., Kim, Y.W., Song, I.H.: Influence of sintering atmosphere and BN additives on microstructure and properties of porous SiC ceramics, *J. Eur. Ceram. Soc.*, **14**, [41], 6925–6933, (2021).
- ²³ Fenetaud, P., Jacques, S.: SiC/SiC ceramic matrix composites with BN interphase produced by gas phase routes: an overview, *Open Ceramics*, **15**, (2023):
- ²⁴ Li, H., Meng, Q., Jin, S., Li, H.: Effect of ball milling parameters on mechanical alloying of Y_2O_3 and Al_2O_3 mixed powders, *J. Changchun Univ. Technol.* (Nat. Sci. Ed.), (01), 1–4, (2007).
- ²⁵ La, P., Ju, Q., Lu, X., Wie, Y., Guo, X.: Microstructure and properties of YAG/ Al_2O_3 composite ceramics prepared by thermite reaction, *J. Lanzhou Univ. Technol.*, **37**, [04], 10–13, (2011).
- ²⁶ Wu, L., Jiang, Y., Qiao, F.: Effect of sintering temperature on mechanical properties of silicon carbide ceramics, *Powder Metall. Technol.*, **28**, [01], 58–60, (2010).
- ²⁷ Guo, Y., Ge, Y., Liu, W. *et al.*: Reactive-sintered low-thermal expansion cordierite ceramic with high stiffness, *J. Ceram. Sci. Tech.*, **15**, [2] 69–78, (2024).
- ²⁸ Zhi-Hua, Y. *et al.*: Thermal shock resistance of *in situ* formed SiC-BN composites, *Mater. Chem. Phys.*, **107**, [2], 476–479 (2007).
- ²⁹ Zeng, X., Sun, R., Yu, S., Xu, J., Wong, C.P.: Research progress and development trends of electronic packaging substrate materials, *J. Integr. Technol.*, **3**, [06], 76–83, (2014).
- ³⁰ Li, X., Zhang, L., Yin, X., *et al.*: Mechanical and dielectric properties of porous Si_3N_4 -SiC(BN) ceramic, *J. Alloy Compd.*, **490**, [1], L40 – L43 (2009).